Earth Planets Space, **58**, 823–830, 2006

An improved double-difference earthquake location algorithm using *sP* phases: application to the foreshock and aftershock sequences of the 2004 earthquake offshore of the Kii peninsula, Japan (M_w=7.5)

Ling Bai[1], Ichiro Kawasaki[1], Tianzhong Zhang[2], and Yuzo Ishikawa[3]

[1]*Disaster Prevention Research Institute, Kyoto University, Gokasho, Uji, 611-0011, Japan*
[2]*Institute of Geophysics, China Earthquake Administration, Beijing 100081, China*
[3]*Matsushiro Seismological Observatory, Japan Meteorological Agency, Matsushiro 381-1232, Japan*

(Received January 3, 2006; Revised February 23, 2006; Accepted March 8, 2006; Online published July 26, 2006)

We have used *sP* phases to improve the hypocentral locations of the earthquakes that occurred offshore southeast of the Kii peninsula in association with the M_w=7.5 mainshock on September 5, 2004. The earthquakes were more than 100 km from the onshore seismic network and, thus, their focal depths were poorly constrained. The *sP* phases were recorded about 7–11 s after the initial *P* phases, with both phases having almost the same apparent velocities. The computation of ray-paths revealed that the arrival times of the later *sP* phases are sensitive to focal depths. We have recalculated the hypocenters and origin times for 36 events with more than six *sP* phase identifications on seismograms recorded at the High Sensitivity Seismograph Network by including *sP* phases in a double-difference earthquake location algorithm, which eliminates the errors introduced by crustal heterogeneity. The relocation results were then compared with those from the Japan Meteorological Agency based on traditional absolute location techniques.

Key words: The 2004 earthquake offshore of the Kii peninsula, foreshock and aftershock sequences, improved double-difference earthquake location algorithm using *sP* phases, Philippine Sea plate.

1. Introduction

Earthquake focal depth is an important parameter for assessing seismic hazard, discriminating natural earthquakes from nuclear explosions, and understanding the tectonic process. However, the determination of the focal depth has been a difficult problem because the arrival time data are generally observed at stations on the surface of the Earth. Many methods of locating earthquakes have been developed to improve the resolution of the focal depth. One such example is the double-difference earthquake location algorithm which eliminates the substantial errors introduced by crustal heterogeneity (Waldhauser and Ellsworth, 2000) and, to a certain extent, produces a more accurate absolute location of earthquakes than traditional methods (Menke and Schaff, 2004). The time separations between the direct arrivals and depth phases can also lead to a more accurate estimation of focal depths (Umino *et al*., 1995; Engdahl *et al*., 1998; Bai *et al*., 2003; Gamage, 2005). Our strategy has been to improve the double-difference earthquake location algorithm using *sP* phases, which provide independent evidence of the absolute focal depths.

The Nankai Trough is one of the best-studied subduction zones in the world (see Nakamura *et al*., 1997; Ishikawa, 2001; Obana *et al*., 2003) and is where the Philippine Sea plate (PHS) is subducting beneath the overriding Eurasia plate with a convergence rate of around 5–6 cm/year (Seno *et al*., 1993). The 2004 earthquake offshore of the Kii peninsula occurred close to the deformation front of the Nankai Trough (Fig. 1). Since seismological stations are mostly located in onshore areas, the insufficient station coverage led to significant uncertainty in the depth determination. Five pop-up type ocean bottom seismometers (OBSs) were initially deployed on September 8 (3 days after the mainshock) at a spacing of about 10 km; beginning on September 14, 25 OBSs were operating in order to cover the whole region of the aftershocks (Sakai *et al*., 2005). Most of the hypocenters determined by the Japan Meteorological Agency (JMA) (Fig. 2(a)) were deeper than 30 km, whereas most of the hypocenters relocated by OBS data (Fig. 2(b)) or by double-difference analyses with direct *P*- and *S*- arrival times (Enescu *et al*., 2005) were shallower than 30 km. However, earthquakes with magnitudes greater than 4 cannot be located accurately using OBS data because of the limited dynamic range of the OBS recording system (Sakai *et al*., 2005).

2. *sP* Depth Phases at Epicentral Distances of 120 to 300 km

With the operation of the High Sensitivity Seismograph Network (Hi-net) throughout Japan, high-quality seismograms enable us to identify depth phases at local epicentral distances for small earthquakes. Distinct later phases (which we call here the *X* phases) were observed for the foreshock and the aftershock sequences associated with the 2004 earthquake offshore of the Kii peninsula at epicentral

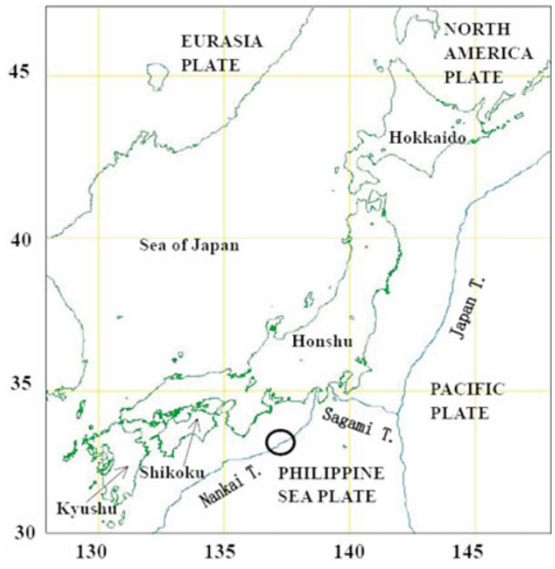

Fig. 1. Map of the Japan Islands showing the location of the 2004 earthquake offshore of the Kii peninsula (the open circle) and the tectonic setting. Curved lines show the Japan Trench, Sagami Trench and Nankai Trench, which are the major plate boundaries in the Japan region.

distances between 120 and 300 km (Fig. 3). The properties of these phases are as follows:

1) They are observed between the direct P- and S- wave arrivals, with a travel time delay of 7–11 s following the P.
2) They are dominant on the vertical-component seismograms.
3) Their apparent velocities are almost the same as those for the direct P waves.
4) Their particle motions are similar to those of the direct P phases.

To investigate the origin of the X phases, we have calculated the travel times using a two-dimensional (2-D) ray-tracing program (Zelt and Smith, 1992). This program uses an efficient numerical solution of ray tracing equations and a simulation of smooth layer boundaries to yield stable inversion results. The 2-D P-wave velocity structure was determined by Nakanishi *et al*. (2002) from an OBS seismic experiment. The S-wave velocities can be computed by a constant Vp/Vs ratio of 2.5 for the sedimentary wedge layer and a Vp/Vs ratio of 1.73 for other layers (Obana *et al*., 2003). The similarity between the observed and the calculated travel times suggests that the X phase is a sP wave, which takes-off upward as a S wave from the focus, converts to a P wave at the water-sediment boundary at a point relatively near the epicenter, then dives into the Earth again (Fig. 4). Distinct sP phases at small epicentral distances were recorded from the foreshock and aftershock sequences of the 2004 earthquake offshore of the Kii peninsula as well as from a large number of offshore events in northeastern Japan (Umino *et al*., 1995; Wang and Zhao, 2005).

3. Earthquake Relocation Method

3.1 Double-difference algorithm for direct *P* and *sP* waves

When there is a dense distribution of earthquakes, the ray paths between the source region and a common station are similar, and thus errors introduced by crustal heterogeneity can be substantially eliminated. A common travel-time difference equation between two events i and j at the same station k is as

$$\frac{\partial t_k^i}{\partial m}\Delta m^i - \frac{\partial t_k^j}{\partial m}\Delta m^j = dr_k^{ij} \tag{1}$$

(after Waldhauser and Ellsworth, 2000). Where t_k^i is the travel time from events i to station k, $\Delta m^i = (\Delta x^i, \Delta y^i, \Delta z^i, \Delta t^i)$ is the change in the hypocentral parameters of event i, and $dr_k^{ij} = (t_k^i - t_k^j)^{\text{obs}} - (t_k^i - t_k^j)^{\text{cal}}$ is the residual between observed and calculated differential travel time between the two events i and j. The partial derivatives of t with respect to m are the components of the slowness vector of the ray connecting the source and receiver measured at the source, which can be written out in full as formulas (2) to (4).

$$\frac{\partial t}{\partial x} = \sin(i_h)\cos(Az)/v \tag{2}$$

$$\frac{\partial t}{\partial y} = \sin(i_h)\sin(Az)/v \tag{3}$$

$$\frac{\partial t}{\partial z} = \cos(i_h)/v \tag{4}$$

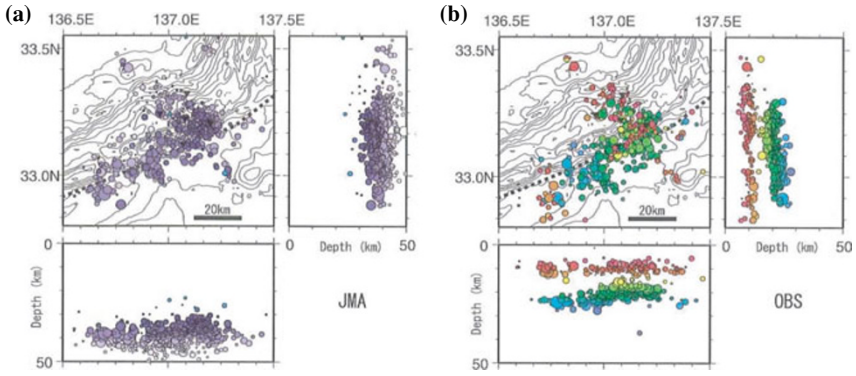

Fig. 2. Comparison between (a) the JMA hypocenters and (b) the hypocenters determined by five OBS instruments (After Sakai *et al*., 2005). Broken lines indicate the Nankai Trough. Most of the hypocenters located by JMA are deeper than 30 km, whereas most of the hypocenters located with the OBS instruments are shallower than 30 km.

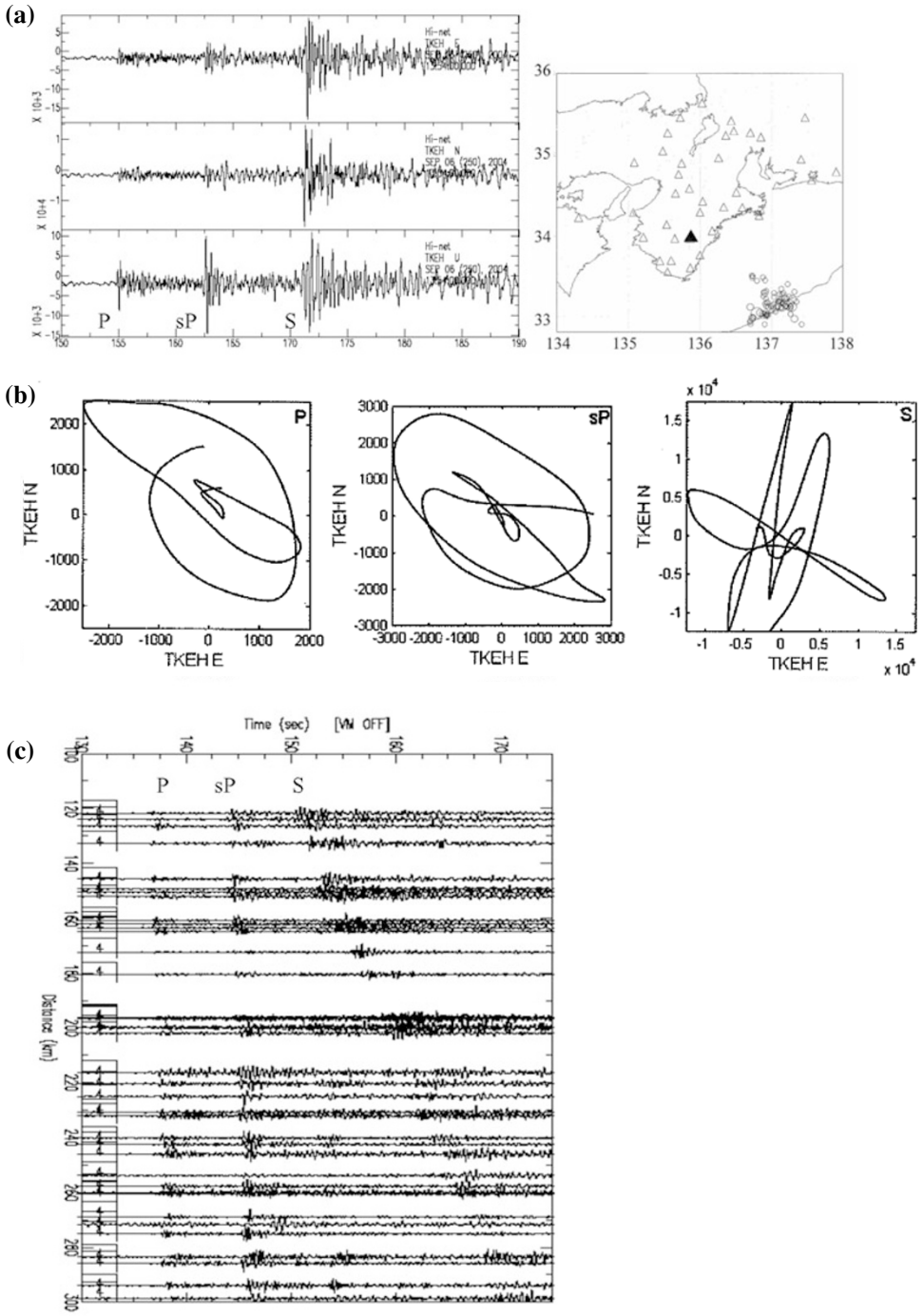

Fig. 3. An example event showing *sP* phases. (a) Three-component seismograms recorded at the Hi-net station N.TKEH, which is indicated by solid triangle in the inset. (b) Particle motions of *P*, *sP*, and *S* waves recorded at the same station, N.TKEH. (c) Recorded section of vertical-component seismograms reduced by 8 km/s. Waveforms are band-pass-filtered from 1 to 4 Hz. This example is event 17 in Table 1.

where v is the velocity, and i_h and Az are the take-off angle and the azimuthal angle from source to station, respectively. Equations (1) to (4) are considered to be the common equations of the double-difference earthquake location algorithm for both the direct P and the sP phases even though their take-off angles (i_h^P and i_h^{sP}) are different.

3.2 Double-difference algorithm including *sP* phases

At regional distances, if a seismic station is far from an earthquake, the take-off angle i_h^P approaches 90° and the corresponding coefficient $\cos(i_h^P)$ is small. Therefore, the equations for the direct waves are not sensitive to focal depths and subsequently lead to large errors in focal depth determination. The calculation of i_h^{sP} is an important step in the improvement of the double-difference earthquake location algorithm using sP phases. The 2-D ray-tracing program of Zelt and Smith (1992) calculates i_h^{sP} using an iterative shooting/bisection search mode while tracing through the velocity structure. The 2-D ray-tracing equations are a pair of first-order ordinary differential equations that can be written in the following form:

$$\frac{dx}{dz} = \tan\theta, \frac{d\theta}{dz} = \frac{(v_z \tan\theta - v_x)}{v} \tag{5}$$

Table 1. Comparison of the location results for 36 earthquakes. The Mj is a local magnitude defined and calculated by JMA. The date and origin time are local time in Japan.

No.	Date	Mj	This study				JMA			
			Origin time (h:min:s)	(λ_E/(°))	(φ_N/(°))	H/km	Origin time (s)	(λ_E/(°))	(φ_N /(°))	H/km
1	2004:09:05	3.5	19:53:45.08	137.21	33.07	19.91	45.06	137.21	33.07	37.78
2	2004:09:05	3.7	19:56:05.04	137.20	33.07	20.51	05.08	137.20	33.07	37.70
3	2004:09:05	4.5	20:15:57.86	137.15	33.11	22.69	57.96	137.14	33.11	39.08
4	2004:09:05	3.6	20:20:20.08	137.20	33.07	17.98	20.18	137.20	33.07	36.43
5	2004:09:05	3.5	20:34:43.32	137.23	33.07	22.52	43.38	137.23	33.08	39.43
6	2004:09:05	4.1	21:36:17.92	136.94	32.99	24.85	18.00	136.94	33.00	39.05
7	2004:09:05	4.0	22:15:39:04	137.09	33.21	27.57	40.16	137.11	33.20	38.21
8	2004:09:05	4.1	22:52:22.16	136.73	32.98	21.57	22.80	136.73	32.98	33.00
9	2004:09:05	3.6	23:01:32.80	136.70	32.99	21.26	32.76	136.70	32.99	37.00
10	2004:09:06	4.3	00:53:19.07	137.13	33.26	15.38	18.89	137.15	33.27	46.56
11	2004:09:06	3.8	01:02:27.27	136.94	33.36	19.78	27.46	136.94	33.37	48.19
12	2004:09:06	4.3	01:06:42.34	136.92	33.22	16.37	42.39	136.92	33.22	40.00
13	2004:09:06	4.2	01:12:24.69	137.02	33.10	16.74	24.72	137.02	33.10	36.00
14	2004:09:06	4.5	01:13:56.01	136.95	33.02	32.13	56.05	136.95	33.02	43.00
15	2004:09:06	4.7	02:34:09.18	137.01	33.07	17.60	09.25	137.01	33.07	36.54
16	2004:09:06	3.9	08:20:49.78	136.89	33.27	16.20	49.81	136.90	33.25	47.05
17	2004:09:06	3.7	13:56:12.41	137.07	33.14	16.35	12.37	137.07	33.13	41.74
18	2004:09:06	4.2	15:35:44.21	137.07	33.11	16.56	44.22	137.07	33.11	37.95
19	2004:09:06	4.1	19:39:46.62	137.21	33.12	20.59	46.84	137.20	33.12	35.15
20	2004:09:06	3.8	23:29:50.28	136.77	32.96	18.85	50.30	136.78	32.95	42.00
21	2004:09:07	3.8	02:23:36.96	136.78	32.96	21.28	37.08	136.78	32.97	37.00
22	2004:09:07	3.6	02:49:21.83	136.73	32.96	18.35	21.82	136.73	32.97	35.00
23	2004:09:07	3.8	10:37:09.08	137.17	33.15	18.86	09.11	137.17	33.15	37.86
24	2004:09:07	3.5	14:45:54.88	137.43	32.92	16.16	54.64	137.43	32.92	42.57
25	2004:09:07	3.7	15:51:49.14	137.43	32.92	17.95	48.84	137.43	32.92	43.34
26	2004:09:08	4.1	02:20:31.50	136.71	32.94	17.13	31.36	136.71	32.93	35.00
27	2004:09:08	3.6	03:58:17.69	136.75	32.94	18.02	17.55	136.75	32.94	38.81
28	2004:09:08	3.6	04:42:50.54	136.82	33.40	16.01	50.46	136.81	33.41	39.29
29	2004:09:09	3.8	00:13:44.76	136.94	33.24	15.68	44.92	136.94	33.24	38.31
30	2004:09:09	4.0	03:50:42.88	137.26	33.11	17.17	42.96	137.26	33.11	43.48
31	2004:09:09	3.5	09:18:51.69	136.70	32.92	16.08	51.66	136.70	32.92	31.56
32	2004:09:10	3.7	11:10:32.91	136.67	33.08	17.61	33.00	136.66	33.07	37.28
33	2004:09:11	3.6	20:04:48.24	136.77	32.88	18.48	48.48	136.77	32.89	35.03
34	2004:09:12	3.5	09:52:54.51	136.79	33.44	15.00	54.39	136.81	33.42	40.85
35	2004:09:13	3.5	13:50:16.34	137.18	33.10	18.16	16.41	137.18	33.10	39.85
36	2004:09:25	3.5	08:51:06.80	136.71	32.90	16.85	06.87	136.71	32.90	36.00

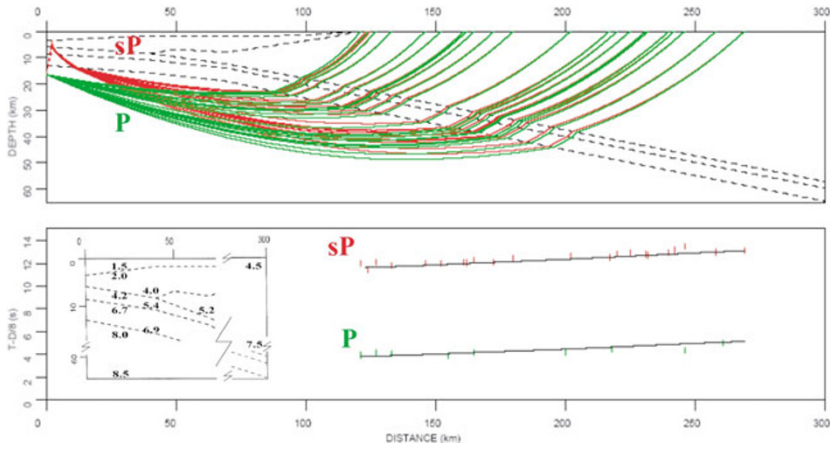

Fig. 4. Ray path diagram of P waves and sP waves (top panel) and comparisons of travel times between the observed values (vertical bars) and the traced values (curves). Inset shows the P-wave velocity model from an OBS seismic experiment. The upper and lower layer velocities are given for each layer, with the exception that a constant velocity was used in the seawater layer. The S-wave velocities are computed by a constant Vp/Vs ratio of 2.5 for the sedimentary wedge layer and 1.73 for other layers. A reduced velocity of 8 km/s has been applied. The example with a focal depth of 21.3 km is event 17 listed in Table 1.

with initial conditions $x = x_0, z = z_0, \theta = \theta_0$ (Cêrvený *et al.*, 1977: equation 3.19'). The variable θ is the angle between the tangent to the ray and the z axis. The z coordinate is the positive downward. The point (x_0, z_0) is the source location, and θ_0 is the take-off angle.

4. Data

According to the JMA catalog, there was a total of 225 earthquakes with magnitudes greater than 3.5 during the period between September 5 and September 30, 2004 (Fig. 5). Among those events, two earthquakes (the M_w=7.3 fore-

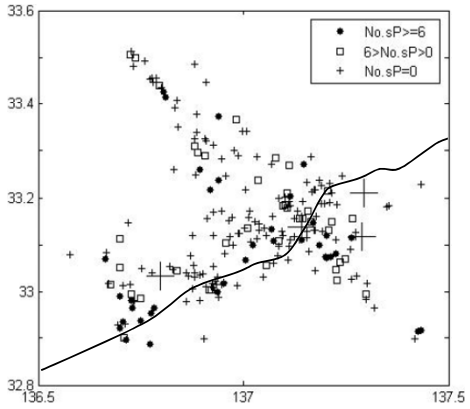

Fig. 5. Epicenter distribution of earthquakes with magnitudes greater than 3.5 in the period between September 5 and September 30, 2004 listed in the JMA catalog. Solid circles indicate events with more than six *sP* phase identifications; open squares. with one to five *sP* phase identifications; pluses, without *sP* phase identifications. Four large pluses indicate events with magnitudes greater than 6. Curved line shows the Nankai Trench.

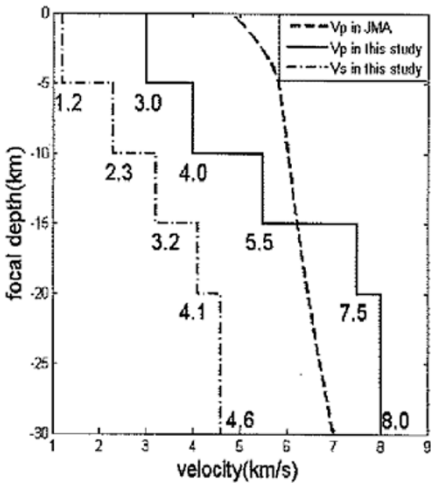

Fig. 6. Comparison of velocity models. Vp is used by JMA (the dotted line); Vp and Vs are used in double-difference analyses (the solid line and the broken line, respectively).

shock and the M_w=7.5 mainshock) had magnitudes larger than M_w=7.0, two (the M_w=6.7 aftershocks) had magnitudes of M_w=6.0–6.9, seven had magnitudes of M_w=5.0–5.9, 68 had magnitudes of M_w=4.0–4.9, and 146 had magnitudes of M_w=3.5–3.9. The arrivals of *sP* waves were identified on seismograms recorded at Hi-net, which has been operated by the Japanese National Research Institute for Earth Science and Disaster Prevention (NIED) since 1999. Of these 225 events, 36 had *sP* phase identifications at more than or equal to six stations (solid circles in Fig. 5), and 39 had *sP* phase identifications at one to five stations (open squares in Fig. 5). For the foreshock and the mainshock, pairs of later *P* and *S* phases were recorded after the initial *P* and *S* phases, which are different from the *sP* phases. The 1-D *P*- and *S*-wave velocity structure (Fig. 6) used in double-difference analyses are derived from Nakanishi *et al.* (2002) and Obana *et al.* (2003).

For the 36 events with more than six *sP* identifications, we obtained hypocenters and origin times by including *sP* phases in the double-difference earthquake location algorithm. There was a total of 144 unknowns for the latitudes, longitudes, depths, and original times of each event, and 2355 equations for *P* waves, 2040 for *S* waves, and 1004 for *sP* waves.

5. Results

The relocation results of the 36 earthquakes are listed in Table 1 and shown in Figs. 7, 8, and 9. The seismic activity started with a M_w=7.3 foreshock on a north-dipping reverse fault plane striking in nearly an east-west direction. After the foreshock, most events took place along the deformation front of the Nankai Trough (Fig. 8(a)). The M_w=7.5 mainshock occurred about 5 h after the foreshock on a multiple faulting with primarily two different fault planes: a northwest-tending strike-slip fault plane and a south-dipping reverse fault plane (Miyoshi and Ishibashi, 2005; Park and Mori, 2005; Satake *et al.*, 2005; Yagi, 2005). After the mainshock, earthquakes extended in both the northwest and southwest directions from the location of the mainshock (Fig. 8(b)). Two major aftershocks occurred on September 7 and September 8, respectively, in a similar location. After the first major aftershock, some small aftershocks seemed to have been distributed at the southeast and southwest of the whole region of aftershocks (Fig. 8(c) and (d)).

The Moho discontinuity in the focal area of the 2004 earthquake offshore of the Kii peninsular is about 13 km in southeast and about 15 km in northwest (Nakanishi *et al.*, 2002). Focal depths of the 36 events relocated in this study range between 15 and 35 km, which are about 15 km shallower than the JMA locations and almost the same depth as the deep branch of the OBS locations (Fig. 9(a)). The focal depths increased with the increases in the observed time

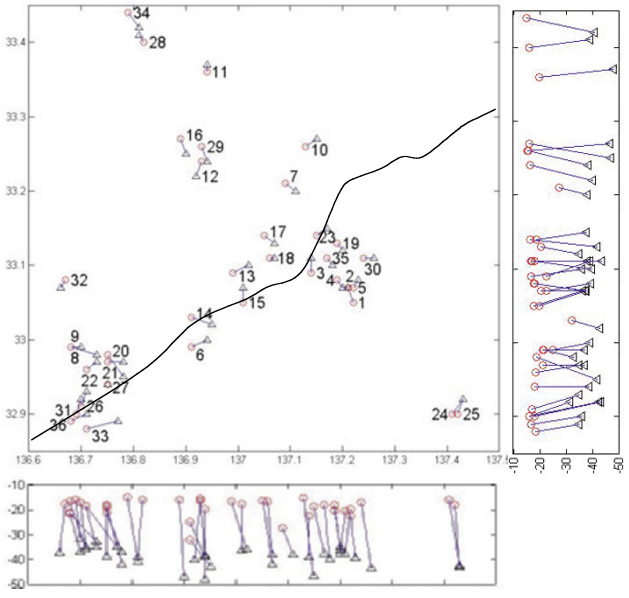

Fig. 7. Comparison between the JMA hypocenters (triangles) and the hypocenters relocated in this study (circles). Curved line indicates the Nankai Trough. Vertical sections along latitude (right) and longitude (lower) are also shown.

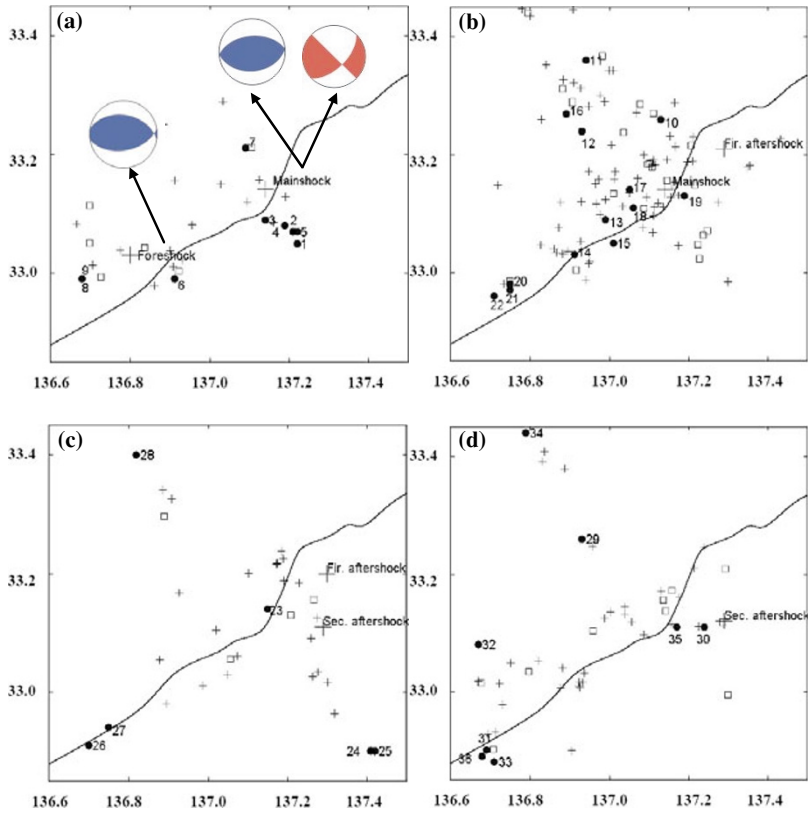

Fig. 8. Map views of epicenters for several time periods: (a) time from the foreshock to the mainshock, (b) time from the mainshock to the first major aftershock, (c) time from the first aftershock to the second major aftershock, (d) time after the second major aftershock. Epicenters of 36 events together with event number are relocated in this study. Focal mechanisms of the foreshock and the mainshock are by Yagi (2005) from teleseismic waveform inversion. Other symbols are the same as those used in Fig. 5.

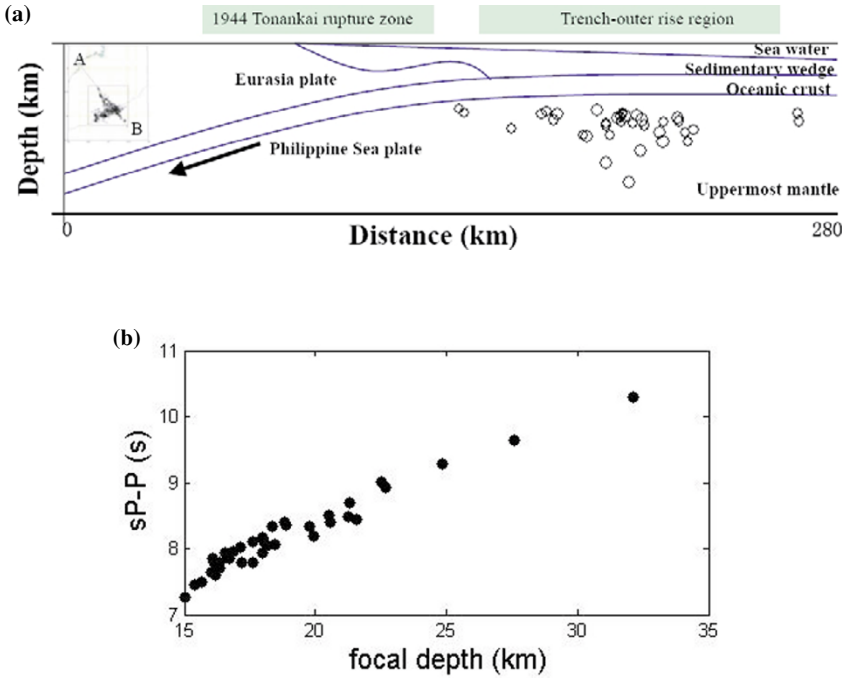

Fig. 9. (a) A cross-section of relocated hypocenters along the plate-subduction direction AB (in the inset) with 2-D velocity boundaries (after Nakanishi *et al.*, 2002). Earthquakes are located in the PHS slab beneath the trench-outer rise region. Coseismic rupture zone of the 1944 Tonankai earthquake estimated by tsunami and geodetic data (Ando, 1975) is shown at the top of the figure. (b) Observed time separations between the *P* and *sP* phases versus focal depths.

separations between the P and sP phases (Fig. 9(b)).

The accuracy of absolute hypocenter locations is generally controlled by several factors, including the accuracy of velocity structure, available phases, arrival-time reading accuracy, and the network geometry (Pavlis, 1986). In this study, the location accuracy was constrained by the double-difference analyses with sP phases. The stations used in this study had an azimuthal gap of about 260°, which meant that the poor network geometry alone would cause mislocations of about 0.25 km in the epicenters and about 1 km in the depths (Bai *et al.*, 2006). All of the stations are located north of the region of the aftershocks, which caused the location errors in the north-south direction to be larger than those for the east-west direction.

6. Discussion and Conclusions

Locating earthquakes in offshore regions is problematic due to the uncertainties in the local velocity structure, the lack of near-source recordings, and poor azimuthal coverage of stations. We included the travel times of the sP phases in the double-difference earthquake location algorithm to improve the accuracy of depth determination. All events were located in the oceanic uppermost mantle. Between the period of the foreshock and the mainshock, events took place along the deformation front of Nankai Trough. After the mainshock, events extended in both the northwest and southwest directions from the location of the mainshock. Following the first major aftershock, some events seemed to be distributed at the southeast and southwest of the whole region of aftershocks.

There might be some uncertainties for identifying later phases, such as the sediment-basement reflections (sdP and pdP), the water-sediment reflections (pP), and the water-surface reflection (pwP) (e.g., Pearce, 1981; Engdahl and Billington, 1986). The sea bed and sea surface usually have a high impedance contrast, and as a result of some complications it could be possible that sP arrives at about the same time as pwP. However, if the amplitude of the later phase between P- and S-wave arrivals is larger than that for P wave, its origin should be S.

The Tonankai earthquake (M_w=8.0) of December 7, 1944 and the Nankai earthquake (M_w=8.2) of December 21, 1946 occurred offshore of southwest Japan in this region. The coseismic rupture zone of the 1944 Tonankai earthquake estimated by tsunami and geodetic data (Ando, 1975) is shown along the top of the Fig. 9(a). Microearthquake activity is low in the rupture area of the Tonankai earthquake, whereas it is higher in trench-outer rise region (Seno, 2005; Sakai *et al.*, 2005, see the top of Fig. 9(a)).

The effective elastic thickness of the PHS in the focal region, estimated from the seafloor age, is about 35 km (Yoshioka and Ito, 2001). Most of the hypocenters located by JMA that are deeper than 35 km might not be reasonable estimates. It is considered that reverse fault events tend to occur prior to, and normal fault events tend to occur after, a large nearby interplate earthquake (Lay *et al.*, 1989). The occurrence of the 2004 earthquake offshore of the Kii peninsula with reverse fault plane in the trench-outer rise region may suggest that the compressional stress is accumulating in the adjacent interplate region and, therefore, there is a potential for future large earthquakes.

Acknowledgments. This research was financially supported by the Sasakawa Scientific Research Grant from the Japan Science Society (17-064). The waveform data used in this study was provided by the Hi-net and collected into CD-ROM by Dr. Shiro Ohmi. Thanks are due to Drs. James Mori, Eric A. Bergman, E. Robert Engdahl, Takuo Shibutani and Kiyoshi Ito for many comments on the manuscript. We are also grateful to the EPS editor and reviewers, Drs. David Schaff and Norihito Umino for constructive suggestions.

References

Ando, M., Source mechanism and tectonic significance of historical earthquake along the Nankai Trough, Japan, *Tectonics*, **27**, 119–140, 1975.

Bai, L., T. Z. Zhang, and H. Z. Zhang, Multiplet relative location approach and waveform correlation correction and their application, *Acta Seismol. Sinica*, **16**, 606–615, 2003.

Bai, L., Z. L. Wu, T. Z. Zhang, and I. Kawasaki, The effect of distribution of stations upon location error accuracy: statistical tests based on the double-difference earthquake location algorithm and the bootstrap method, *Earth Planets Space*, **58**, e9–e12, 2006.

Cêrvený, V., I. Molotkov, and I. Pšencîk, Ray method in seismology, University of Karlova, Prague, Czechoslovakia, 1977.

Enescu, B., J. Mori, and S. Ohmi, Double-difference relocations of the 2004 off the Kii peninsula earthquakes, *Earth Planets Space*, **57**, 357–362, 2005.

Engdahl, E. R. and S. Billington, Focal depth determination of central Aleutian earthquakes, *Bull. Seismol. Soc. Am.*, **76**, 77–93, 1986.

Engdahl, E. R., R. Hilst, and R. Buland, Global teleseismic earthquake relocation with improved travel times and procedures for depth determination, *Bull. Seismol. Soc. Am.*, **88**, 722–743, 1998.

Gamage, S. S., Offshore double-planed shallow seismicity in the northeastern Japan forearc region revealed by sP depth phase, Master thesis, Tohoku Univ., 96 pp, 2005.

Ishikawa, Y., The shape of the Philippine Sea slab, *Journal of Geography*, **110**, 592–601, 2001 (in Japanese with English abstract).

Lay, T., D. H. Christensen, L. Astiz, and H. Kanamori, Temporal variation of large intraplate earthquakes in coupled subduction zones, *Phys. Earth Planet. Inter.*, **54**, 258–312, 1989.

Menke, W. and D. Schaff, Absolute earthquake locations with differential data, *Bull. Seismol. Soc. Am.*, **94**, 2254–2264, 2004.

Miyoshi, T. and K. Ishibashi, A tectonic interepretation of NW-SE strike-slip faulting during the 2004 off the Kii peninsula earthquakes, Japan: Probable tear of the Philippine Sea plate, *Earth Planets Space*, **57**, 1115–1120, 2005.

Nakamura, M., H. Watanabe, T. Konomi, S. Kimuta, and K. Miura, Characteristic activities of subcrustal earthquakes along the outer zone of southwestern Japan, *Annu. Disaster Prevention Res. Inst.*, 40 B-1, 1997 (in Japanese with English abstract).

Nakanishi, A., N. Takahashi, J.-O. Park, S. Miura, S. Kodaira, Y. Kaneda, N. Hirata, T. Iwasaki, and M. Nakamura, Crustal structure across the coseismic rupture zone of the 1944 Tonankai earthquake, the central Nankai Trough seismogenic zone, *J. Geophys. Res.*, **107**, doi: 10.1029/2001JB000424, 2002.

Obana, K., S. Kodaira, Y. Kaneda, K. Mochizuki, and M. Shinohara, Microseismicity at the seaward updip limit of the western Nankai Trough seismogenic zone, *J. Geophys. Res.*, **108**, doi: 10.1029/2002JB002370, 2003.

Park, S. -C. and J. Mori, The 2004 sequence of triggered earthquakes off the Kii Peninsula, Japan, *Earth Planets Space*, **57**, 315–320, 2005.

Pavlis, G. L., Appraising earthquake hypocenter location errors: a complete practice approach for single-event locations, *Bull. Seismol. Soc. Am.*, **76**, 1699–1717, 1986.

Pearce, R. G., Complex P waveforms from a Gulf of Aden earthquake, *Geophys. J.*, **64**, 187–200, 1981.

Sakai, S., T. Yamada, M. Shinohara, H. Hagiwara, T. Kanazawa, K. Obana, S. Kodaira, and Y. Kaneda, Urgent aftershock observation of the 2004 off the Kii peninsula earthquake using ocean bottom seismometers, *Earth Planets Space*, **57**, 363–368, 2005.

Satake, K., T. Baba, K. Hirata, S. Iwasaki, T. Kato, S. Koshimura, J. Takenaka, and Y. Terada, Tsunami source of the 2004 off the Kii Peninsula earthquakes inferred from offshore tsunami and coastal tide gauges,

Earth Planets Space, **57**, 173–178, 2005.

Seno, T., S. Stein, and A. E. Gripp, A model for the motion of the Philippine Sea plate consistent with NUVEL-1 and geological data, *J. Geophys. Res.*, **98**, 17941–17948, 1993.

Seno, T., The September 5, 2004 off the Kii Peninsula earthquakes as a composition of bending and collision, *Earth Planets Space*, **57**, 327–332, 2005.

Umino, N., A. Hasegawa, and T. Matsuzawa, *sP* depth phase at small epicentral distances and estimated subduction plate boundary, *Geophys. J. Int.*, **120**, 356–366, 1995.

Waldhauser, F. and W. L. Ellsworth, A double-difference earthquake location algorithm: method and application to the Northern Hayward Fault, California, *Bull. Seismol. Soc. Am.*, **90**, 1353–1368, 2000.

Wang, Z. and D. P. Zhao, Seismic imaging of the entire arc of Tohoku and Hokkaido in Japan using P-wave, S-wave and *sP* depth-path data, *Phys. Earth Planet. Inter.*, **152**, 144–162, 2005.

Yagi, Y., http://iisee.kenken.go.jp/staff/yagi/eq/Japan20040905/Japan20040905_1-j.html, 2005 (in Japanese).

Yoshioka, S. and Y. Ito, Lateral variations of effective elastic thickness of the subducting Philippine Sea plate along the Nankai trough, *Earth Planets Space*, **53**, 261–273, 2001.

Zelt, C. A. and R. B. Smith, Seismic traveltime inversion for 2-D crustal velocity structure, *Geophys. J. Int.*, **108**, 16–34, 1992.

L. Bai (e-mail: bai@rcep.dpri.kyoto-u.ac.jp), I. Kawasaki, T. Zhang, and Y. Ishikawa